JOURNAL OF APPLIED ELECTROCHEMISTRY **26** (1996) 693–701

Recovery of pickling effluents by electrochemical oxidation of ferrous to ferric chloride

P. F. MARCONI, V. MEUNIER, N. VATISTAS

Dipartimento di Ingegneria Chimica, Chimica Industriale e Scienza dei Materiali, Università di Pisa, via Diotisalvi 2, 56100 Pisa, Italy

Received 10 April 1995; revised 24 January 1996

The characteristics of the effluents from the preparatory pickling step of zinc plating are presented and the various methods of oxidizing ferrous to ferric chloride are briefly considered. An electrochemical oxidation method is proposed to recover these effluents by using an electrochemical cell with three-dimensional electrodes and an anion selective membrane. A near exhausted hydrochloric acid solution was used as catholyte. The experimental data obtained from the proposed cell show a faradic yield of 100% and easy control of the parasitic reactions. The three-dimensional anode was modelled and it is shown that at high values of current only the felt entrance region works efficiently.

Nomenclature

A	membrane surface (cm^2)
a	specific felt surface (cm^{-1})
ΔC	concentration difference ($mol\,dm^{-3}$)
D	average diffusion coefficient through the membrane ($cm^2\,s^{-1}$)
i_n	felt wall flux of species ($mol\,cm^{-2}\,s^{-1}$)
j	total current density ($A\,cm^{-2}$)
j_0	exchange current density ($A\,cm^{-2}$)
j_1	current density in matrix ($A\,cm^{-2}$)
j_2	current density in felt solution ($A\,cm^{-2}$)
j_n	transfer current density ($A\,cm^{-2}$)
L	thickness of felt electrode (cm)
L_m	thickness of membrane (cm)
M	transport of ferrous and ferric ions through the membrane (mol)
N	superficial flux of ion reactant ($mol\,cm^{-2}\,s^{-1}$)
u	superficial fluid velocity ($cm\,s^{-1}$)
x	distance through felt electrode (cm)
R	universal gas constant ($8.3143\,J\,mol^{-1}\,K^{-1}$)
T	absolute temperature (K)
t	time (s)

Greek letters

α_a, α_c	anodic and cathodic transfer coefficient
η	local overpotential ($\eta = \Phi_1 - \Phi_2$) (V)
κ	conductivity of solution ($mS\,cm^{-1}$)
μ	solution viscosity (Pa s)
ρ	solution density ($g\,cm^{-3}$)
σ	conductivity of solid matrix ($mS\,cm^{-1}$)
Φ_1	electrostatic potential in matrix phase (V)
Φ_2	electrostatic potential in solution (V)

1. Introduction

Effluents from the pickling step of surface preparation in zinc plating are acid solutions with a high concentration of ferrous chloride. Although these solutions do not have practical applications and require some treatment for disposal, ferric chloride solutions are widely employed in the organic chemical industry as oxidizing agents and are especially used in waste treatment plants as flocculants.

Gaseous chlorine is often used to oxidize concentrated solutions of ferrous to ferric chloride. This gas–liquid redox reaction needs special safety measures, due to the presence of the highly toxic gaseous chlorine. For this reason, the oxidation reaction is usually conducted in the neighbourhood of the gaseous chlorine production plants. Rarely are the effluents from a pickling plant available; instead of effluents, concentrated solutions of ferrous chloride obtained from scrap iron, and concentrated solutions of hydrochloric acid, may be used to produce ferric chloride. This entails an additional cost, and more generally, it leaves unsolved the problem of the disposal of pickling effluents.

An electrochemical method is proposed to oxidize the effluents of concentrated ferrous chloride to ferric chloride using an electrochemical cell composed of two half-cells separated by an anion selective membrane. A low concentration solution of hydrochloric acid is chosen as catholyte such as may be derived from organic chlorination processes [1] or otherwise. The electrochemical procedure presents several advantages: it does not require hazardous reactants, it is modular in nature and can easily be adapted to different capacities. It is also suitable in locations where pickling effluents are produced near waste water treatments plants.

The characteristics of pickling effluents are reported and the various oxidizing methods are considered. The proposed electrochemical methods, the cell and

0021-891X

the experimental results are discussed and the local distribution of current is obtained by modelling the three-dimensional anode.

2. Pickling effluents and commercial ferric chloride solution

Zinc is widely used as a coating for steel because it provides low-cost corrosion protection. It protects steel even when the deposit of zinc is porous or contains small breaks. The pickling pretreatment of steel produces an effluent that is an acid solution of concentrated ferrous chloride (18–27% by weight $FeCl_2$ and 1–4% HCl) [2, 3].

The commercially available ferric chloride solutions used as flocculants have an average composition given in Table 1. Their production usually occurs in two steps: first, the concentrated hydrochloric acidic reacts with scrap iron to give an acid ferrous chloride solution; second, the gaseous chlorine oxidizes the ferrous to ferric chloride [4].

The total concentration of $FeCl_2$ and $FeCl_3$ is lower in pickling pretreatment effluents than in commercial ferric chloride solution, so the concentration of ferrous or ferric chloride has to be increased. This can be accomplished either by partial evaporation of the solution, or by adding concentrated hydrochloric acid and scrap iron to the pickling effluents. The latter is often a cheaper procedure.

3. Chemical oxidation of the pickling pretreatment effluents

The oxidizing agents for the ferrous ions proposed in the literature [5–11] are oxygen (from air), ozone, gaseous chlorine etc. The oxidation of ferrous to ferric chloride with oxygen is a gas–liquid reaction which occurs at low pH, according to the reaction [5–9]:

$$2FeCl_2 + \tfrac{1}{2}O_2 + 2HCl \longrightarrow 2FeCl_3 + H_2O \quad (1)$$

Similarly, oxidation with ozone, occurs according to the reaction:

$$2FeCl_2 + O_3 + 2HCl \longrightarrow 2FeCl_3 + H_2O + O_2 \quad (2)$$

The above reactions show: (i) that water production occurs, and (ii) that additional water is introduced by the use of hydrochloric acid aqueous solution. In this way a low concentration ferric chloride solution is obtained and an evaporation step is required to eliminate a large amount of water. For this reason we have not considered the use of these oxidizing agents to transform the pickling pretreatment effluents into commercial ferric chloride solution.

Table 1. Composition of the $FeCl_3$ solution

Species	*Concentration* /mol dm^{-3}	*Concentration* /g (g solution)$^{-1}$
$FeCl_2$	0.0562	0.005
$FeCl_3$	3.5140	0.400
HCl	0.1954	0.005

The oxidation of ferrous to ferric chloride using gaseous chlorine occurs according to the redox reaction [10]:

$$FeCl_2 + \tfrac{1}{2}Cl_2 \longrightarrow FeCl_3 \quad (3)$$

This gas–liquid reaction is fast [11] and does not introduce additional water into the solution, but strict safety measures are required during transport and handling of gaseous chlorine. Therefore, this process is carried out in practice only in the vicinity of a chlorine production plant.

4. Electrochemical oxidation of pickling pretreatment effluents

The electrochemical oxidation of ferrous to ferric ions in pickling pretreatment effluents occurs at the anode of the cell [12–14]. The standard potentials of some possible reactions at the anode are:

$$Fe^{2+} = Fe^{3+} + e^- \qquad E^0_{Fe^{2+}/Fe^{3+}} = -0.77\,V \quad (4)$$

$$2H_2O = O_2 + 4H^+ + 4e^- \qquad E^0_{H_2O/H^+} = -1.23\,V \quad (5)$$

$$2Cl^- = Cl_2 + 2e^- \qquad E^0_{Cl^-/Cl_2} = -1.36\,V \quad (6)$$

The comparison among the above standard potentials shows that the oxidation of ferrous to ferric iron is thermodynamically more favoured than the oxidation of chloride ion, while the water decomposition is unlikely to occur due to the high overpotential of oxygen production on the graphite anode. Gaseous chlorine production may occur, but only when the ferrous ion concentration reaches very low values.

The catholyte to be used depends mainly on availability: an exhausted hydrochloric acid solution may be used and, if possible, the pickling pretreatment effluent itself. In this case the standard potential of the reduction reactions occurring at the iron cathode are:

$$2H^+ + 2e^- = H_2 \qquad E^0_{H^+/H_2} = +0.00\,V \quad (7)$$

$$Fe^{2+} + 2e^- = Fe \qquad E^0_{Fe^{2+}/Fe} = -0.44\,V \quad (8)$$

So reduction of ferrous ions and hydrogen production occur simultaneously. The latter reaction reduces the pH of the solution and allows the precipitation of ferrous ions. Some preliminary experimental work was done to establish if hydrogen evolution at the cathode is significant or not.

Whatever catholyte is used, the chloride ions needed by the anolyte have to be supplied by the catholyte itself; selective transport of chloride ions through a membrane, due to its specific selectivity, performs this goal.

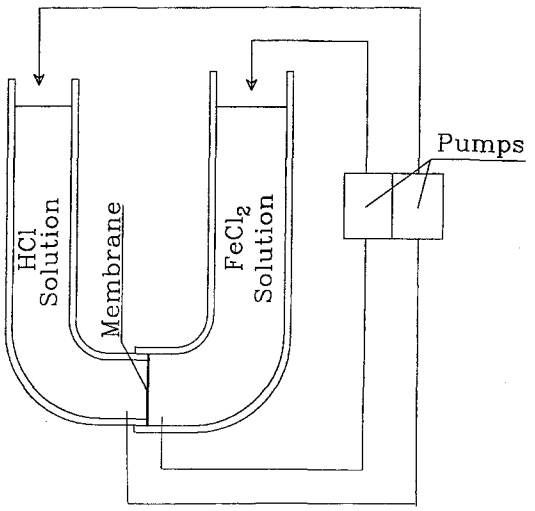

Fig. 1. Apparatus for preliminary experiments

5. Preliminary experiments

The proposed electrochemical procedure requires a membrane which is highly selective and stable in acid conditions. To test these properties of the membrane a simple apparatus was used, made up by two PVC tubes as in Fig. 1. The IONAC–MA 3475 anionic selective membrane placed at the end of the smaller tube had a free surface of 1.13 cm^2. The membrane was previously immersed for three hours in a 10% by weight NaCl solution then soaked in distilled water, as suggested by the suppliers. After complete swelling, the thickness of the membrane was 0.5 mm.

Two different solutions were used for the two half-cells: (i) a solution of 68 ml, 2.8 mol dm^{-3} in $FeCl_2$ and (ii) a solution of 15 ml, 0.5 mol dm^{-3} in HCl, while two external recycles assured homogeneity of the concentrations in each half-cell. The overall concentration of ferrous and traces of ferric ions in the solution, that initially contained only HCl, were determined at the end of each experiment. The concentration against time data (Table 2), indicate that the selectivity and stability of the membrane remain constant for at least 100 h.

The data obtained allow calculation of average diffusion coefficient of the ferrous and ferric ions D, through the membrane, by using Fick's law within the membrane:

$$D = \frac{L_m M}{A \Delta C t} \tag{9}$$

where A is the membrane surface, ΔC is the difference in total ferrous and ferric concentration through the membrane, M the transport of ferrous and ferric ions through the membrane, L_m the thickness of membrane and t the duration of the experiment. The obtained value of the average diffusion coefficient for the ferrous and ferric ions, D, was 2.2×10^{-8} cm^2 s^{-1}, that is about one thousand times smaller than the diffusion coefficient in solution. The small value obtained demonstrates a negligible diffusion of iron ions through the membrane.

Table 2. $FeCl_2$ and $FeCl_3$ concentration against time from membrane tests

Test no.	*Duration* /min	*Concentration* /mol dm^{-3}
1	880	0.0022
2	505	0.0013
3	3920	0.0093
4	3920	0.0100

The same apparatus was adopted to establish if the hydrogen evolution reaction was significant when the effluent was used as catholyte. An iron electrode was used as cathode and a graphite electrode as anode. It was assumed that the effluent was concentrated and contained 3.2 mol dm^{-3} in $FeCl_2$, 0.2 mol dm^{-3} in HCl. Solutions of this composition were used for the experimental work reported hereafter. Recycling was used, as before, to keep the anolyte and the catholyte homogeneous and to remove the ferric ions from the anode and any hydrogen from the cathode.

A calomel reference electrode and an EG&G PAR potentionstat/galvanostat (model 273) were used to establish the potential between the reference and working electrode. It was observed that the production of hydrogen was considerable at the cathode, even for low values of overpotential, while at the anode the oxidation of ferrous to ferric ions occurred without gaseous chlorine production. This preliminary experimental work showed that, using the effluent solution, it was difficult to obtain the reduction of ferrous ion at the cathode without hydrogen evolution. Thus, a low concentration solution of hydrochloric acid was adopted as catholyte.

6. Physical and transport properties of the anolyte

The anolyte initially contains $FeCl_2$, HCl and traces of $FeCl_3$. During the oxidation process its composition and physical properties change. Conductivity, density and viscosity were measured in solutions of various concentrations of $FeCl_2$ and $FeCl_3$ with a concentration 0.2 mol dm^{-3} in HCl at a constant temperature of 25 °C. The different solutions were obtained by mixing fractions of the two following solutions: (i) 3.35 mol dm^{-3} in $FeCl_2$, 0.2 mol dm^{-3} in HCl and (ii) 3.23 mol dm^{-3} in $FeCl_3$, 0.2 mol dm^{-3} in HCl.

An Amel 123 conductivity meter was used to measure the conductivity, an Ubbelohde type viscometer gave the viscosity, and an AP PAAR DMA 58 density meter gave the density. The values of viscosity are the mean value of three different measurements.

The data obtained for the conductivity, density and viscosity are reported in Table 3: linear relationships fit the density and the conductivity data well

$$\rho = 1.3169 + 0.0420\,C \tag{10}$$

$$\kappa = 56.745 - 10.391\,C \tag{11}$$

while a quadratic relationship fits the viscosity

$$\mu = 2.6997 + 0.7656\,C + 0.3281\,C^2 \tag{12}$$

where, ρ is the density, κ is the conductivity, μ is the viscosity and C is the $FeCl_3$ concentration.

Table 3. Physical and transport data

Conc. $FeCl_2$ /mol dm^{-3}	*Conc. $FeCl_3$* /mol dm^{-3}	*Conductivity* /mS cm^{-1}	*Density* /g cm^{-3}	*Viscosity* /Pa s × 10^3
3.350	0.000	57.0	1.3155	2.656
3.009	0.334	54.0	1.3321	2.993
2.665	0.666	51.0	1.3460	3.456
2.320	0.994	48.0	1.3580	3.767
1.984	1.322	39.0	1.3737	4.280
1.644	1.644	38.5	1.3847	4.857
1.311	1.966	36.0	1.3987	5.384
0.980	2.286	33.0	1.4126	6.161
0.651	2.604	30.0	1.4265	6.952
0.323	2.921	27.0	1.4403	7.578
0.000	3.230	24.0	1.4525	8.583

7. Experimental details

The experimental setup (Fig. 2), comprised the cell, two reservoirs (one containing 100 ml of anolyte and another reservoir containing 400 ml of catholyte), two variable-speed peristaltic pumps and two flow-meters. Two cylindrical half-cells were designed for the electrodes and the flow-through cell was built in plexiglass. The IONAC-MA 3475 anionic selective membrane separated the anolyte and catholyte (active membrane surface 10.18 cm^2) and two O-ring seals were placed between the half-cells and the membrane to prevent electrolyte leakage. The half-cells were held in compression with bolts and an external metal frame. The reference potential was measured using a Luggin located close to the anode; other electrodes of platinum were located at different positions in the cell to measure the potential.

The anode was a 3.6 cm diameter, 0.5 cm thick graphite felt (Sigratherm GFD5, specific surface 240 cm^{-1}, void volume fraction 0.95). The cathode was a stack of five sheets of expanded metal (Costacurta, AISI 304) perpendicular to the direction of the catholyte flow. The expanded metal was characterized by various parameters: pitch p_1 and p_2, metal thickness h_1, total thickness h_2 as shown in Fig. 3. Two different types were used: (i) small type; p_1 = 6.0 mm, p_2 = 2.5 mm, h_1 = 0.30 mm, h_2 = 0.35 mm, specific surface 17.78 cm^{-1}, void volume fraction 0.82, total cathode surface 633 cm^2 and (ii) large type; p_1 = 8.0 mm, p_2 = 4.0 mm, h_1 = 0.50 mm, h_2 = 1.10 mm, specific surface 5.36 cm^{-1}, void volume fraction 0.78, total cathode surface 480 cm^2.

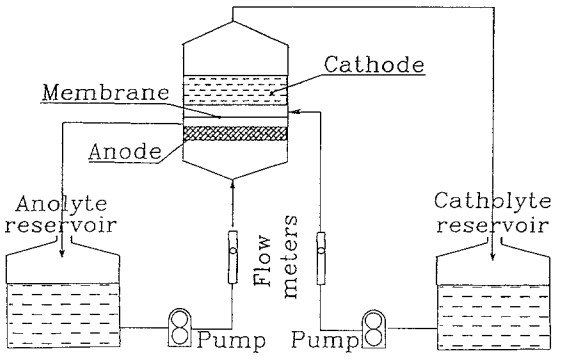

Fig. 2. Experimental setup.

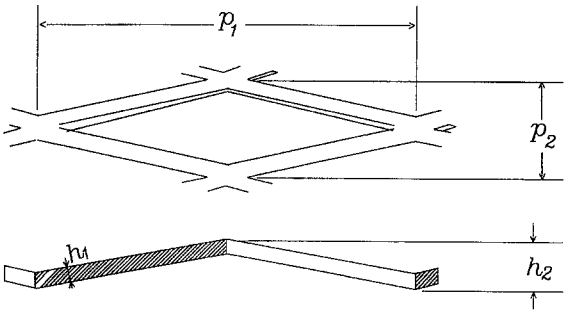

Fig. 3. Schematic representation and parameters of expanded metal cathode; pitch $p_1 \times p_2$, metal thick h_1, whole thick h_2.

Anolyte simulating a pickling pretreatment effluent was employed in the experiments. Its composition was 3.2 mol dm^{-3} $FeCl_2$, 0.2 mol dm^{-3} HCl. Catholyte simulating exhausted acid chloride solution was employed and its composition was 1.0 mol dm^{-3} HCl. Anolyte and catholyte were electrolysed at a steady anode to cathode potential (8 V), while both electrolytes were continuously circulated through the cell and reservoirs. The anolyte superficial fluid velocity was between 0.3 and 0.5 cm s^{-1} and the catholyte between 1.3 and 2.0 cm s^{-1}.

The pH of the catholyte was obtained during the experiments using a Hanna HI 8417 pH meter and the ferrous concentration in the anolyte was sampled and measured. Current and charge were also measured during the experiments, allowing the faradic yield to be calculated. The potential in the anolyte close to the membrane (over the anode), was measured using a calomel electrode, while three platinum electrodes were used to measure the potential in the anolyte under the anode, and the potential in the catholyte over and under the cathode. A 14 channel analogue/digital 16 bit Cole–Parmer MAC-14 system was used.

8. Experimental results and discussion

A constant potential of 8 V was applied between anode and cathode: for this potential the complete oxidation of ferrous to ferric ions occurred in about three hours. At the anolyte the ferrous chloride decreased, this caused a colour change. Initially the solution was translucent green; during the experiment it gradually became dark brown. At the end of the experiment an unexpected colour variation was observed: from a dark brown to a lighter translucent brown. The viscosity of the anolyte increased as expected during the experiments, because ferric chloride solution is more viscous than ferrous chloride solution.

Typical data for the measured ferrous concentrations as well as the theoretical concentration, calculated by the measured charge against time, is reported in Fig. 4. This figure shows that the faradic yield obtained experimentally was a little more than one hundred per cent. This unexpected value was

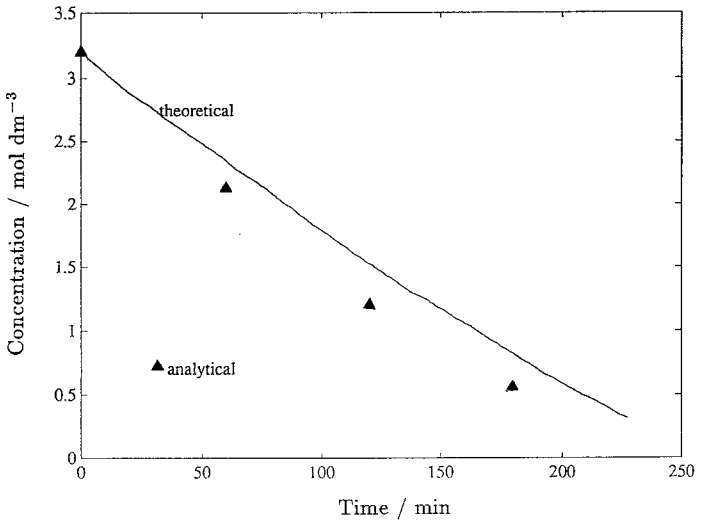

Fig. 4. Analytical and theoretical ferrous concentration during an experimental run.

probably due to the oxidizing effect of the oxygen in the air during the three hour experiment. During the experiments the HCl concentration of the catholyte decreased and production of hydrogen occurred at the cathode.

The two types of used expanded metal showed different behaviour. The first type with small mesh did not allow easy removal of hydrogen bubbles which accumulated within the expanded metal and in the region between the cathode and the membrane and they were removed cyclically. This created high current fluctuations due to the fluctuation in the active cathode surface, which did not occur in the case of large mesh cathode as shown in Fig. 5. The same Figure shows a similar cathodic overpotential in both cases.

The anodic overpotentials for the two previous cases are reported in Fig. 6, the overpotential being higher in the case of high current (i.e., 0.8 V), which is not enough to produce gaseous chlorine. The observed decrease of the anodic overpotentials, during the experiment, is principally due to the current decreasing during the experiment. The chloride ion oxidation to gaseous chlorine occurs at the end of the experiment when all the ferrous ions are oxidized; moreover, this reaction starts sharply with a high production of gaseous chlorine. Thus to establish the end of the oxidation process is easy; by direct observation of the gaseous chlorine produced or by the sharp increase in the anodic overpotential, as shown in Fig. 6 for the case of large type cathode.

The potential drop through the selective membrane is reported in Fig. 7 for the two cases of small and large type cathode. A higher value is observed in the case of the small type cathode, which is due to the reduction of the active surface of the membrane by the adherent hydrogen bubbles. In both cases a high potential drop through the anion selective membrane is observed, which is due to the high value of current density. During the experiment an increase of the potential drop through the membrane despite the decreasing of the current is observed, which is due to the decreasing concentration of the chloride ions in the catholyte.

The effect of ion concentration in the catholyte on the current and potential drop through the membrane has been observed experimentally (Fig. 8), adding some acid to a quite exhausted catholyte solution,

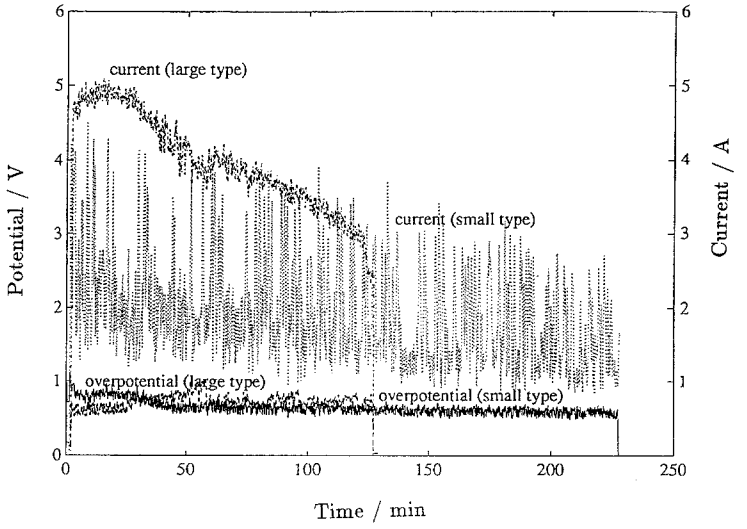

Fig. 5. Cathodic overpotential (and current) against time, using small and large type cathodes.

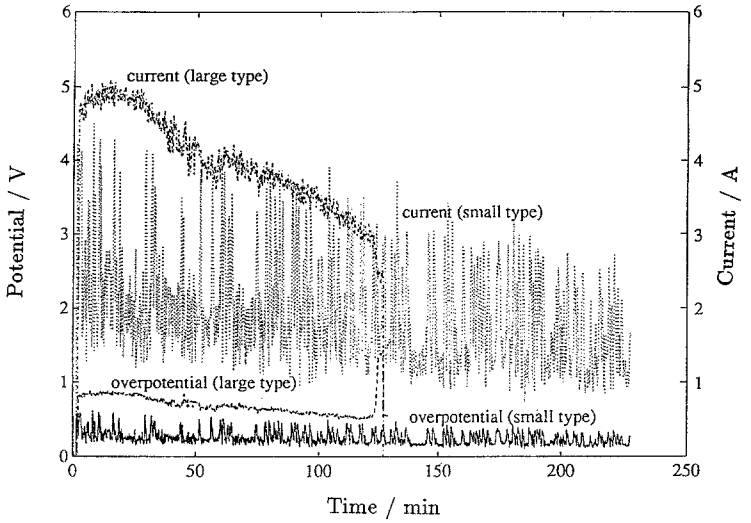

Fig. 6. Anodic overpotential (and current) against time, using small and large type cathodes.

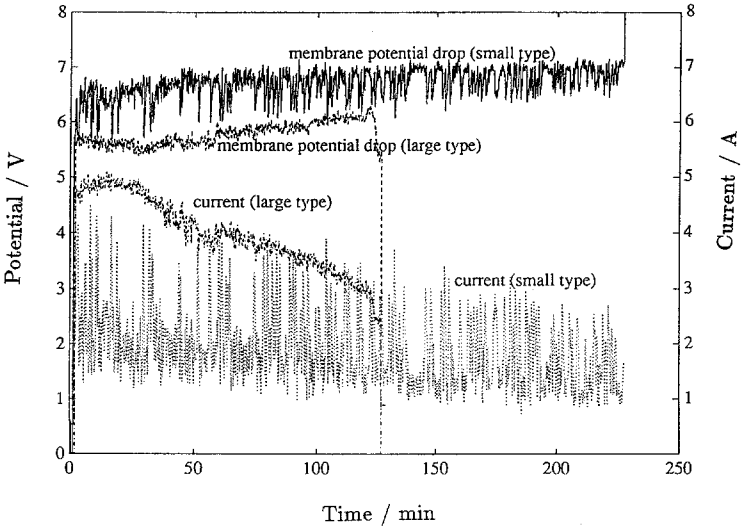

Fig. 7. Membrane potential drop (and current) against time, using small and large type cathodes.

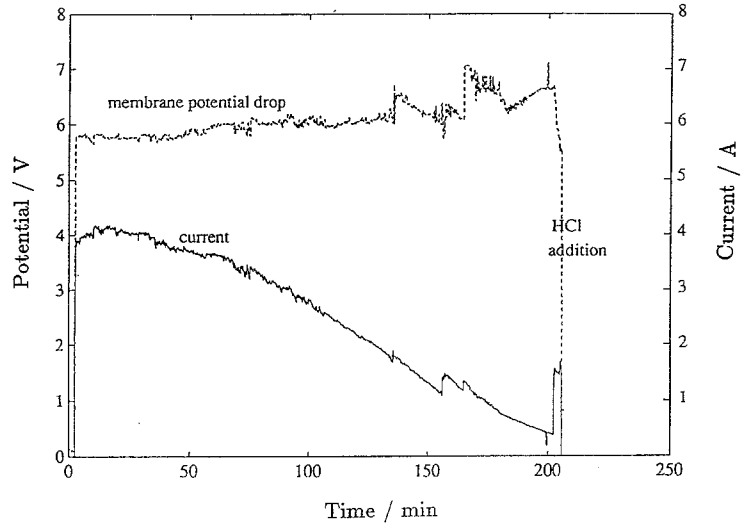

Fig. 8. Effect of the addition of HCl during the experiment on membrane potential drop and current.

thus increasing HCl concentration to about 0.25 mol dm^{-3}. The experimentally obtained current and potential drop through the membrane allows a calculation of the resistance of the anion selective membrane ($R = V/I$; where V is the measured potential drop, I is the measured current). The resistance is reported in Fig. 9. A high increase in the resistance is observed when the concentration of HCl became less than 0.1 mol dm^{-3}.

The electrolytes during the experiments reached

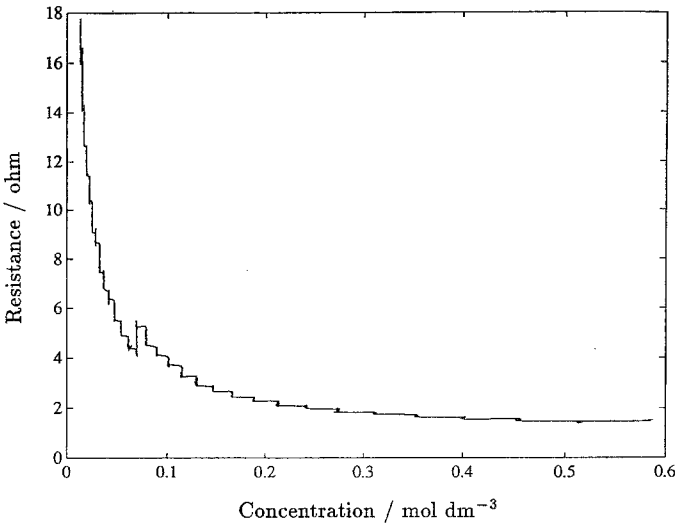

Fig. 9. Resistance of the selective membrane against HCl concentration during an experimental run.

40 °C when the room temperature was 26 °C. This increase was certainly due to the Joule effects. The high potential applied at the membrane, combined with the high current density, exposes the membrane to high stress. The same membrane was used for more than 12 h (four experiments) and a change in its colour was observed at the cathode side, which covered about a third of the whole active surface of the selective membrane. Despite its colour change the membrane maintained its integrity (as revealed by the inspection under a Zeiss SV stereomicroscope) as well as its selectivity (as revealed by the faradic yield data).

9. Model

The experimental results showed that the cathodic overpotential is fairly constant while the anodic overpotential increases with current. The prediction of the performance of the anode for larger system is made possible by modelling the three-dimensional anode to obtain the relationships between the local distribution of transfer current and geometric characteristics of the graphite felt.

The anodic reaction at the flow through graphite felt anode with parallel current and fluid flow was modelled with the following restrictions: (i) the model is one-dimensional; (ii) the graphite felt anode is of length L and has an isotropic porosity, ϵ, and specific felt surface, a, which remain constant in time; (iii) the hydrodynamics are characterized by the superficial velocity u; (iv) simultaneous side reactions do not occur; (v) the matrix conductivity is much higher than the solution conductivity ($\sigma \gg \kappa$).

Only one material balance is required and, at steady state conditions, this may be expressed as

$$\frac{dN}{dx} = i_n a \tag{13}$$

where N is the superficial flux of reactant ions, x is the distance through felt electrode, i_n is the felt wall flux of reactant.

In the system the anolyte is recycled and during the flow through the anode only a small fraction of ferrous ions is oxidized to ferric; thus a constant concentration of the solution in the felt was assumed. With this assumption the current density j_2 in the felt solution is governed by Ohm's law

$$j_2 = -\kappa \frac{d\Phi_2}{dx} \tag{14}$$

where Φ_2 is the electrostatic potential in solution.

The transfer current density is due to the anodic oxidation

$$\frac{dj_2}{dx} = j_n a \tag{15}$$

where j_n is the transfer current density due to the anodic reaction and is related to the felt wall flux of reactant i_n:

$$j_n = -nFi_n \tag{16}$$

The high matrix conductivity ($\sigma \gg k$) assures that the electrostatic potential in the matrix phase (Φ_1) is nearly constant and the local overpotential $\eta = \Phi_1 - \Phi_2$ is obtained by Equation 14:

$$\frac{d\eta}{dx} = \frac{d(\Phi_1 - \Phi_2)}{dx} = -\frac{d\Phi_2}{dx} = \frac{j_2}{\kappa} \tag{17}$$

In general the transfer current density due to the oxidation may be approximated by the Butler–Volmer equation

$$j_n = j_0 \left[\exp\left(\frac{-\alpha_c F}{RT}\eta\right) - \exp\left(\frac{\alpha_a F}{RT}\eta\right) \right] \tag{18}$$

where j_0 is the exchange current density, α_a is the anodic transfer coefficient, α_c is the cathodic transfer coefficient, R is the universal gas constant and T is the absolute temperature.

The equation for the overpotential distribution results by combining Equations 14–18:

$$\frac{d^2\eta}{dx^2} = -\frac{j_0 a}{k} \left[\exp\left(\frac{-\alpha_c F}{RT}\eta\right) - \exp\left(\frac{\alpha_a F}{RT}\eta\right) \right] \tag{19}$$

In our experiments a large electrode polarization was

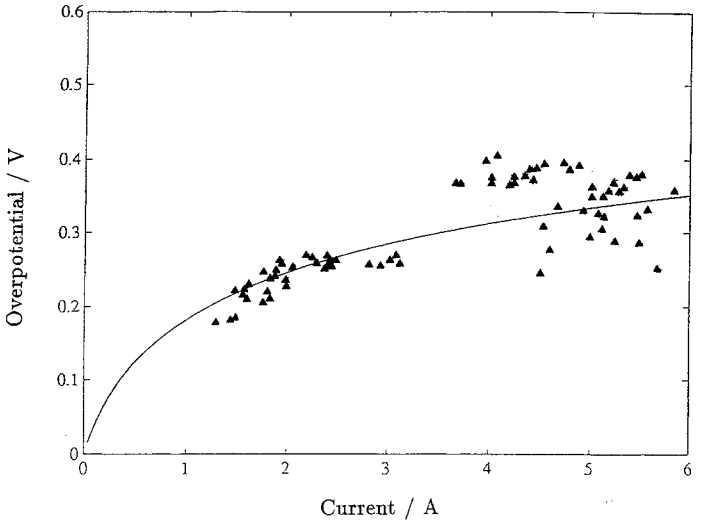

Fig. 10. Theoretical and experimental results of the $(\eta_L - \eta_0)$ against current ($\alpha_a = 0.5$).

used and in this case Equation 19 becomes [15]:

$$\frac{d^2\eta}{dx^2} = 2\frac{j_0 a}{\kappa}\sinh\left[\frac{\alpha_a nF}{RT}\eta\right] \tag{20}$$

The boundary conditions required are that at $x = 0$ (at the felt exit) the electronic current density j_1 is equal to the total current density j and $j_2 = 0$; while at $x = L$ (at the felt entrance), $j_1 = 0$ and $j = j_2$:

$$\frac{d\eta}{dx} = \frac{j_1}{\sigma} = \frac{j}{\sigma} \approx 0 \quad \text{at} \quad x = 0$$

$$\frac{d\eta}{dx} = \frac{j_2}{\kappa} = \frac{j}{\kappa} \quad \text{at} \quad x = L$$

The approximate solution of the Equation 20 at the condition of large electrode polarization is [15]:

$$\exp\left(\frac{\alpha_a nF}{2RT}(\eta_0 - \eta)\right) = \cos\left[\exp\left(\frac{\alpha_a nF}{RT}\eta_0\right)\left(\frac{\alpha_a nF}{2RT}\right)^{1/2}\left(\frac{j_0 a}{\kappa}\right)^{1/2} x\right] \tag{21}$$

while the total current density is obtained by the use of the second boundary condition:

$$\left(\frac{\alpha_a nF}{2RT}\right)\frac{L}{\kappa} j = \arccos\exp\left(\frac{\alpha_a nF}{2RT}(\eta_0 - \eta)\right) \times \tan\left[\arccos\exp\left(\frac{\alpha_a nF}{2RT}(\eta_0 - \eta_L)\right)\right] \tag{22}$$

Fig. 10 shows the $(\eta_L - \eta_0)$ against current derived from Equation 22, as well as the experimental results.

A more practical point, obtained by the proposed model, is the distribution of the local transfer current density, j_n, defined directly by the equation of the local polarization curve:

$$j_n = 2j_0\sinh\left(\frac{\alpha_a nF}{2RT}\right)\eta \approx j_0\exp\left(\frac{\alpha_a nF}{2RT}\eta\right) \tag{23}$$

Combining Equations 21 and 23 the ratio of the transfer current densities at the felt entrance $j_{n,L}$ and

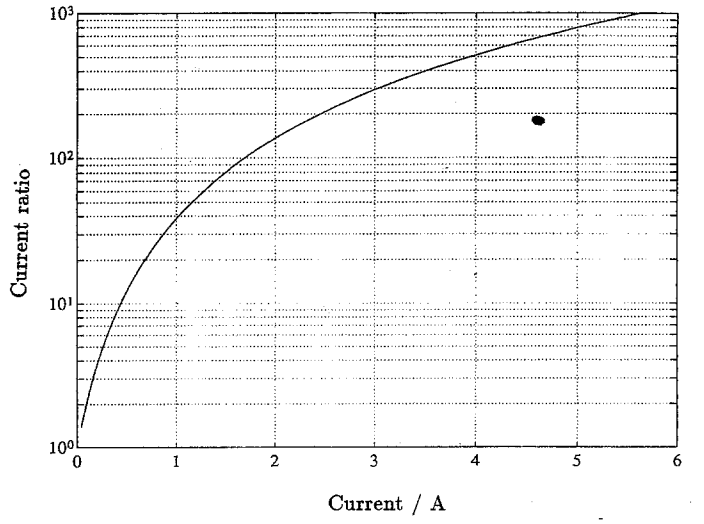

Fig. 11. Transfer current ratio $j_{n,L}/j_{n,0}$ against current.

at the felt exit $j_{n,0}$ is obtained:

$$\frac{j_{n,L}}{j_{n,0}} = \frac{1}{\cos^2\left[\exp\left(\frac{\alpha_a nF}{RT}\eta_0\right)\left(\frac{\alpha_a nF}{2RT}\right)^{1/2}\left(\frac{j_0 a}{\kappa}\right)^{1/2} L\right]}$$

$$= \frac{1}{\exp\left(\frac{\alpha_a nF}{RT}(\eta_0 - \eta_L)\right)} \quad (24)$$

Fig. 11 shows that this ratio increases with increasing current, so that at high current values only the felt entrance region works efficiently.

Conclusions

An electrochemical method was investigated to oxidize ferrous to ferric chloride of an effluent deriving from the preparatory pickling step of zinc plating. The method proposed used a cell with an anion selective membrane and an almost exhausted acid chloride solution as catholyte.

The experimental results show that: (i) a complete oxidation of ferrous to ferric chloride is easily achieved; (ii) a full faradic yield is obtained; (iii) a sharp increase in anodic overpotential occurs when gaseous chlorine production starts, indicating the end of the oxidation process; (iv) the resistance of the selective membrane increases sharply when HCl concentration becomes less than $0.1\,\mathrm{mol\,dm^{-3}}$; (v) modelling of the three-dimensional anode shows that at high values of current only the felt entrance region works efficiently.

Acknowledgement

The research described here was carried out within the frame of the Strategic Project for Innovative Chemical Technologies of the Italian C.N.R.

References

[1] Kirk-Othmer, 'Encyclopedia of Chemical Technology', vol. 7, John Wiley & Sons, New York (1969) p. 659.
[2] J. B. Mohler, 'Electroplating and Related Processes', Chemical Publishing Co., New York (1969) p. 200.
[3] 'Metal Handbook', vol. 5, 9th edn., American Society for Metals (1989) p. 65.
[4] 'Chlorure Ferrique 40% en Solution', Solvay & Cie SA, Rue du Prince Albert, 44. B-1050 Bruxelles/Brussels (1991).
[5] A. Solcova, J. Subrt, J. Vins, F. Hanousek, V. Zapletal and J. Tlaskal, *Collect, Czech. Commun.* **46** (1981) 3049.
[6] B. Matseevskii and D. Feldman, *Kin. Katal.* **14** (1973) 921.
[7] A. Gorshkov and M. Reibakh, *Zh. Prikl. Khim.* **47** (1974) 649.
[8] B. Matseevskii, L. Markov and S. Chernaya, *Latu. PSR Zinat. Akad. Vestis. Kim. Ser.* (1979) 339.
[9] B. Matseevskii, S. Chernaya, *ibid.* (1980) 439.
[10] V. Sysoeva, *Zh Prikl. Khim.* **44** (1971) 2558.
[11] H. Hikita, S. Asai, H. Ishikawa and Y. Saito, *Chem. Eng. Sci.* **30** (1975) 607.
[12] M. Ehrenfreund and J. Leibenguth, *Bull. Soc. Chim. Fr.* **7** (1972) 2590.
[13] N. Smolyag, V. Astashko, I. Zharskii, *Vestsi. Akad. Navuk BSSR. Ser. Khim.* **2** (1987) 56.
[14] Y. Naumov, V. Kucherenko and V. Flerov, *Electrokhimiya* **18** (1982) 1098.
[15] I. Roušar, K. Micka and A. Kimla, 'Electrochemical Engineering II', Parts D–F, Elsevier, Amsterdam (1986) pp. 124–36.